

Spin splitting and switching effect in a four-terminal two-dimensional electron gas nanostructure

Zijiang Wang,¹ Jianhong He,^{1,2} and Huazhong Guo^{1, a)}

¹⁾*College of Physical Science and Technology, Sichuan University, Chengdu 610064, China*

²⁾*National Institute of Measurement and Testing Technology, Chengdu 610021, China*

(Dated: 3 September 2022)

We have studied the spin-splitting effect in a four-terminal two-dimensional (2D) electron gas system with two potential barriers generated by two surface metal gates and an external perpendicular magnetic field. The calculations show that by tuning the voltage applied on the gates, the injected spin-unpolarized current can be split into different spin currents with a high efficiency. The split currents flow out of the geometry from different output leads separately. The spin freedom of the outputs can be controlled by simply tuning voltage on gates. This phenomenon is a result of the combination of three effects - the potential barriers, Zeeman splitting and edge current. Furthermore, by tuning the voltage on gates, the outflow spin of current in one terminal can be switched. Therefore, these features open up a possibility for making a spin filter or a switcher device by applying the four-terminal 2D electron gas system.

The manipulation of spin is a significant issue for spintronics. In the spin transistor proposed by Datta and Das¹, spin-polarized electrons are injected into the semiconductor from a ferromagnet, and by tuning the spin-orbit interaction (SOI), the spin of electrons is manipulated in a desired manner. However, the conductivity mismatch between the semiconductor and ferromagnet leads to a low efficiency of the spin injection, less than 0.1%². To solve this problem, one approach is to inject the spin-polarized current from the magnetic semiconductor³. By using this method, the injection efficiency of the device is reported to be 90%⁴. Another approach is to use the SOI to achieve spin filters without ferromagnets. Several spin filters were proposed by using this method, e.g., quantum dots⁵, semiconductor nanowires⁶, quantum point contacts (QPC)⁷.

Recently an antidot in a quantum wire was proposed as a spin filter/switcher⁸. The operating method to control the spin freedom is based on the effect of resonant backscattering from one edge state into another through localized quasibound states, combined with the effect of Zeeman splitting of the quasibound states in adequately high magnetic field. The author of Ref. 8 expected that by varying parameters of the system, e.g., the magnetic field, the Fermi energy, the antidote size, the conductance of the device could be tuned such that the current in one lead could be due exclusively to spin-up or spin-down electrons.

In this letter, we propose a method to create a spin splitter/switcher. To split different spin current, we need at least three terminals, one for the input current, and another two terminals for different output spin currents. From experimental point of view, varying gate voltage is more convenient than varying magnetic strength. In order to control the spin currents of the three outputs, we utilize two gates on two the conduction channels. The existence of edge current arising from Landau levels has been testified in a semiconductor heterostructure⁹. In the ballistic transport regime, we use the gate-controlled potential barriers, combined with Zeeman splitting effect and edge current to control the spin freedom of the outputs. In a word, we design a four-terminal nanostructure with two surface metal gates, and show that by tuning the voltage of gates, the injected spin-unpolarized current can be split into different spin current with a high efficiency, and flow out of the geometry from different terminals. Furthermore, by tuning the voltage of gates, the outflow spin can be switched.

^{a)}Electronic mail: guohuazhong@scu.edu.cn

We consider the 2D electron gas in a four-terminal system depicted in Fig. 1. The scattering region consists of three parts. The first part is a horizontal narrow long strip at the top of the region, which is slightly curved around $x \sim 450\text{nm}$ to 800nm . The second part is a mirror-symmetrical strip about the x -axis. Finally the third part is a half ring for just connecting the upper and lower parts. The whole geometry is mirror-symmetrical about the x -axis. Contact 2 acts as the injector of spin-unpolarized electronic current and the other three contacts act as outputs.

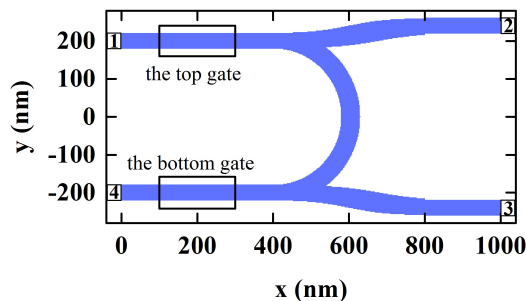


FIG. 1. Schematic of the four-terminal nanostructure with two rectangular gates. Four contacts are numbered from 1 to 4. The unpolarized current is injected from Contact 2.

The 2D electron gas locates at the depth of d beneath the surface of the heterojunction, and two rectangle metal gates on the surface are defined by $l_1 < x < r_1$, $b_1 < y < t_1$ and $l_2 < x < r_2$, $b_2 < y < t_2$ respectively. These gates are located above the branches connected with Contact 1 and Contact 4 respectively, as depicted in Fig. 1. They are mirror-symmetrical about the x -axis. By applying voltages on these gates, we can control the electrochemical potential in the region beneath the gates.

When external magnetic field $\mathbf{B} = (0, 0, -B)$ is applied on the electron gas plane, the Hamiltonian in the system is given by:

$$H = \left[\frac{\mathbf{P}^2}{2m^*} + U(\mathbf{r}) \right] \mathbf{1} + \frac{1}{2} g \mu_B B \sigma_z \quad (1)$$

where $\mathbf{P} = \hbar \mathbf{k} + e \mathbf{A}$, $\mathbf{k} = -i \nabla$, $\mathbf{A} = (-By, 0, 0)$ is the vector potential, m^* is the effective conduction-band electron mass, $\mathbf{1}$ is the 2×2 unit matrix, g is the effective Lande factor, μ_B is the Bohr magneton, and σ_z is the z th Pauli matrix. The second term in Eq. (1) describes the spin-dependent Zeeman split energy. We assume that the confinement in the z direction is so strong that the electrons occupy the ground state due to quantum size effect along this direction. Therefore the confinement potential energy $U(\mathbf{r})$ is given by:

$$U(\mathbf{r}) = U_c(x, y) + U_c(z) + U_g(x, y) \quad (2)$$

where $U_c(x, y)$ is the confinement potential energy in the x - y plane, which is described by the hard-wall confinement in the x - y plane, $U_c(z)$ is the confinement potential energy in z direction, which confines electrons in the x - y plane, and $U_g(x, y)$ is the potential energy aroused by surface gates. According to J. H. Davies model¹⁰, in a depth of d , the potential $\phi(x, y, d)$ aroused by a rectangle gate defined by $l < x < r$, $b < y < t$ can be calculated analytically. For our system with two gates, we have:

$$U_g(x, y) = -e\phi_T(x, y, d) + [-e\phi_B(x, y, d)] \quad (3)$$

where index T denotes the top gate, index B denotes the bottom gate and d is the depth of 2D electron gas. When the gate voltage is negative, potential barrier for electrons will be formed in the channel underneath the gate, which will block electrons from passing through the channel. In the following, We use V_T to denote the top gate voltage and V_B to denote the bottom gate voltage. In our model, the leads' directions are parallel to the x -axis. We perform the numerical calculation within the frame of tight-binding approximation by

using the Kwant package¹¹. The Hamiltonian has to be discretized on grids ($x_\mu = \mu a, y_\nu = \nu a, \mu, \nu = 1, 2, 3, \dots$) with lattice constant a . We introduce the discrete representation of the spinor as follows: $|\Psi(x_\mu, s_\mu, y_\nu, s_\nu)\rangle = (|\varphi^\uparrow(x_\mu, y_\nu)\rangle, |\varphi^\downarrow(x_\mu, y_\nu)\rangle)^T = |\Psi_{\mu,\nu}\rangle$, where s_μ is the spin index ($\mu = \uparrow, \downarrow$), $(\dots)^T$ denotes the matrix transposition. The discretized Hamiltonian is then given by:

$$H = \sum_{\mu,\nu} \left\{ [4t + U_g(x_\mu, y_\nu)] \mathbf{1} + \frac{1}{2} g \mu_B B \sigma_z \right\} |\Psi_{\mu,\nu}\rangle \langle \Psi_{\mu,\nu}| - \sum_{\mu,\nu} (t' \mathbf{1} |\Psi_{\mu+1,\nu}\rangle \langle \Psi_{\mu,\nu}| + t \mathbf{1} |\Psi_{\mu,\nu+1}\rangle \langle \Psi_{\mu,\nu}| + H.c.) \quad (4)$$

where $t = \hbar^2 / (2m^* a^2)$, $t' = t \exp(-i(e/\hbar) B y_\nu a)$.

Considering the four-terminal system, the spin dependent current of spin up ($\sigma = \uparrow$) and spin down ($\sigma = \downarrow$) electrons can be calculated by Büttiker formula¹²:

$$I_p^\sigma = \sum_q G_{pq}^\sigma (V_p - V_q) \quad (5)$$

where p and q are terminal index ($p, q = 1, 2, 3, 4$), G_{pq}^σ is the conductance of spin σ from terminal q to p , V_p is the voltage on Contact p . In our model Contact 2 acts as the injector of electronic current, and other contacts act as outputs. As Contact 2 acts as the injector of electrons, $V_2 < 0$. We treat Contact 1, 3 and 4 as equivalent and without loss of generality, set $V_1 = V_3 = V_4 = 0$. Therefore Eq. (5) reduces to:

$$\begin{aligned} I_1^\sigma &= -G_{12}^\sigma V_2 \\ I_2^\sigma &= (G_{21}^\sigma + G_{23}^\sigma + G_{24}^\sigma) V_2 \\ I_3^\sigma &= -G_{32}^\sigma V_2 \\ I_4^\sigma &= -G_{42}^\sigma V_2 \end{aligned} \quad (6)$$

We focus on the outputs, i.e., terminal 1, 3 and 4. According to Equation (6), we only have to obtain G_{12}^σ , G_{32}^σ , and G_{42}^σ . We assume that $|V_2|$ is so small that the potential change in the scattering region induced by V_2 can be neglected. According to Landauer-Büttiker formula at zero temperature, the conductance can be written as:

$$G_{ij}^\uparrow = \frac{e^2}{h} (T_{ij}^{\uparrow\uparrow} + T_{ij}^{\uparrow\downarrow}) \quad (7)$$

$$G_{ij}^\downarrow = \frac{e^2}{h} (T_{ij}^{\downarrow\downarrow} + T_{ij}^{\downarrow\uparrow}) \quad (8)$$

where $T_{ij}^{\sigma\tau}$ is the probability of transmission between terminal j and terminal i . When $\sigma = \tau$, $T_{ij}^{\sigma\tau}$ is the probability of transmission of electron with the spin conservation. On the other hand, when $\sigma \neq \tau$, $T_{ij}^{\sigma\tau}$ is the probability of transmission of electron with a spin flip. Considering the spin-dependent conductance, we calculate the spin polarization by the current polarization:

$$P_{ij} = G_{ij}^\uparrow - G_{ij}^\downarrow \quad (9)$$

In the calculations, if not stated otherwise, we adopt following geometric parameters: width of each lead $W_l = 40\text{nm}$, width of each strip $W_s = 40\text{nm}$, radius of the inner half circle of the half ring $R = 180\text{nm}$, width of the ring channel $W_r = 50\text{nm}$, center of the ring $x_r = 400\text{nm}$ and $y_r = 0$, length of the scattering region $L = 1000\text{nm}$, geometric parameters of the top surface gate $l_1 = 100\text{nm}$, $r_1 = 300\text{nm}$, $b_1 = 160\text{nm}$, $t_1 = 240\text{nm}$, depth of the 2D electron gas plane $d = 50\text{nm}$, lattice constant $a = 2\text{nm}$, Fermi energy $E_F = 8\text{meV}$. The distance between Contact 2 and 4 d_s is calculated by $d_s = 2(R + W_s/2) = 400\text{nm}$. In our model the two surface gates are mirror-symmetrical about the x -axis. We choose the material parameters corresponding $\text{In}_{0.5}\text{Ga}_{0.5}\text{As}$, i.e., $m^* = 0.0465m_0$, where m_0 is the electron rest mass, and $g = -8.97$. The magnetic strength is $B = 1.5\text{T}$ in the $-z$ direction.

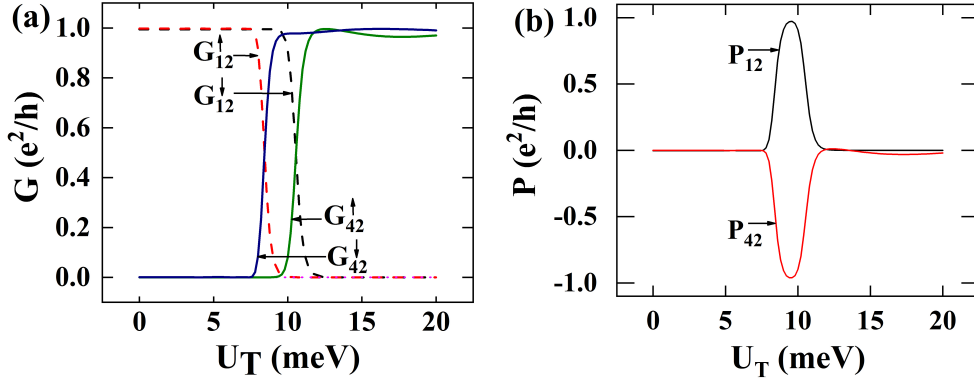


FIG. 2. (a) The conductances G_{12}^σ , G_{32}^σ , and G_{42}^σ ($\sigma = \uparrow, \downarrow$) as the function of U_T while the bottom gate voltage V_B remains zero. Although not labeled, conductances G_{32}^\uparrow and G_{32}^\downarrow remain zero. (b) Polarizations P_{12} and P_{42} as the function of U_T while the bottom gate voltage V_B remains zero. The magnetic strength is $B=1.5\text{T}$ in the $-z$ direction.

In this section, we present results for ballistic transport and discuss the physics of spin polarization in our nanostructure. Without loss of generality, firstly we discuss the relationship between the spin conductances and the top gate voltage V_T . For convenience, we define the potential energy $U_T = -eV_T$ (with a negative sign for electrons), and the potential energy $U_B = -eV_B$, where index T denotes the top gate and B denotes the bottom gate. As the spin-unpolarized current is injected from Contact 2, we present the conductances G_{12}^σ , G_{32}^σ , and G_{42}^σ ($\sigma = \uparrow, \downarrow$) (Fig. 2(a)) and polarizations P_{12} and P_{42} (Fig. 2(b)) as the function of U_T while the bottom gate voltage V_B remains zero. The Fermi energy ensures that only a spin-up mode and a spin-down mode are allowed to be injected into the nanostructure.

Although not labeled in Fig. 2(a), conductances G_{32}^\uparrow and G_{32}^\downarrow remain zero in the range from 0 to 20 meV. We see that in a narrow U_T interval, when increasing U_T , G_{12}^\uparrow (G_{12}^\downarrow) rapidly declines from e^2/h to 0. This decrease is induced by the reflecting effect of the potential barrier brought by the top gate. The threshold energy when the decrease of G_{12}^\uparrow occurs, which is about 9.4 meV, is larger than that when the decrease of G_{12}^\downarrow occurs, which is about 7.6 meV. In the same U_T regime, when the conductance of spin-up electrons is still large, most of the spin-down electrons are already reflected by the potential barrier. The difference between the two threshold energies can be attributed to the splitted subband structure induce by the Zeeman term, i.e., the $g\mu_B B\sigma_z/2$ term in the Hamiltonian. The energy of spin-down subband is lower than that of spin-up subband. This leads to a difference between the probabilities of transmission of spin-up and spin-down electrons for a same potential energy U_T . This effect gives rise to a nonzero spin polarization as shown in Fig. 2(b), where P_{12} and P_{42} are calculated by Equation (9). In addition, the decrease of G_{12}^\uparrow (G_{12}^\downarrow) is accompanied by the increase of G_{42}^\uparrow (G_{42}^\downarrow). This simultaneity illustrates that the electrons reflected by the potential barrier brought by the top gate mostly flow to Contact 4. This effect is caused by the Lorentz force induced by the magnetic field. As the magnetic induction is in the $-z$ direction, the electronic current flow is shifted to the right boundary of the channel in the flowing direction. Thus almost all the electrons reflected flow along the inner boundary of the half ring and to the Contact 4.

We assume that the injected electronic current from Contact 2 is spin-unpolarized. While U_B remains zero and U_T is not zero, the currents in the Contact 1 and 4 are spin-polarized when there is a difference between the probabilities of transmission of two spins in the channel area with a potential barrier, which is due to the spin Zeeman splitting. The electrons reflected by the potential barrier mostly flow to Contact 4 due to the Lorentz force and the electrons do not come out from Contact 3. According Equation (6) and the sum rule, assuming that no electrons are reflected to Contact 2, we have: $(G_{12}^\uparrow + G_{32}^\uparrow + G_{42}^\uparrow)V_2 = (G_{21}^\uparrow + G_{23}^\uparrow + G_{24}^\uparrow)V_2 = I_2^\uparrow = I_2^\downarrow = (G_{21}^\downarrow + G_{23}^\downarrow + G_{24}^\downarrow)V_2 = (G_{12}^\downarrow + G_{32}^\downarrow + G_{42}^\downarrow)V_2$. As

$G_{32}^\uparrow = G_{32}^\downarrow = 0$, after simplifying the equation above, we have: $G_{12}^\uparrow + G_{42}^\uparrow = G_{12}^\downarrow + G_{42}^\downarrow \rightarrow G_{12}^\uparrow - G_{12}^\downarrow = -(G_{42}^\uparrow - G_{42}^\downarrow)$, i.e., the sign of P_{12} and P_{42} are opposite (see Fig. 2(b)). When U_T is over 12meV and P_{12} is zero, P_{42} only deviates a little from zero. The reason may be that a very small part of spin-up electrons is reflected to Contact 2. This small deviation will disappear when the magnetic field is strong enough. Anyway, it is not important in our discussion. From Fig. 2(b), we can see that in our energy range of U_T , $|P_{42}|$ ($|P_{12}|$) reaches a maximum when U_T is approximately 9.5meV. This point corresponds to the point in Fig. 2(a) when the spin-down current is mostly reflected by the potential barrier and the spin-up current just starts to be reflected. The maximum $|P|$ ($|P_{12}|$) is close to e^2/h , about $0.97e^2/h$.

While U_B remains zero, the sign of P_{42} remains unchanged in our energy range of U_T . With the exploit of both the two gates, the sign of P_{42} can be reversed. Fig. 3(a) shows P_{42} as the function of both U_T and U_B . We can see that P_{42} is divided into three regions: a negative region, a positive region and the rest region where P_{42} is about zero. Around the boundary between regions, P_{42} is changed sharply with varying U_T or U_B . As the bottom gate is geometrically equivalent to the top gate, the effect of the bottom gate on the spin current in the bottom channel is similar. The electrons reflected by the potential barrier brought by the bottom gate flow to the Contact 3 along the lower boundary of the bottom horizontal channel due to the Lorentz force. The shape of the negative region is formed by the collective effect of the top and bottom gates. The essence is that the potential energy U_T is in a range where the reflected spin-down electrons exceeds the reflected spin-up electrons, while the potential energy U_B must not exceed 9.5meV so as not to entirely reflect spin-down electrons by the potential brought by the bottom gate. Similarly, the positive region is formed when the potential energy U_T exceeds the threshold energy when the spin-up electrons start to be reflected so as to flow to Contact 4 and the potential energy U_B is in the same range where the reflected spin-down electrons exceeds the reflected spin-up electrons.

We notice that the electrons flow through the nanostructure without spin-flip incidents, but the total spin of electrons coming out from Contact 4 can be reversed by changing U_T and U_B . These electrons originate from the injector - Contact 2. Electrons cannot be reflected to Contact 2 due to the Lorentz force. As electrons injected from Contact 2 are spin-unpolarized, according to sum rule, the total spin of electrons coming out from Contact 1 and 3 must be complementary to the spin of electrons coming out from Contact 2. This will lead to $P_{42} = -(P_{12} + P_{32})$. We present the sum of P_{12} and P_{32} in Fig. 3(b). We can see that the calculation results are consistent with our derivation. We also present the results for P_{12} and P_{32} alone in Fig. 3(c) and Fig. 3(d). We can see that in Contact 1 and 4 alone, the total spin cannot be reversed.

To illustrate the electronic current, we calculate the total spin density s_z (Fig. 4) in the nanostructure for point A and B in Fig. 3(a). The s_z of spin-up electrons is positive while the s_z of spin-down electrons is negative. We can see that electrons injected from Contact 2 are closer to the right boundary of the channel due to the external magnetic field. At point A, $P_{42} \approx -0.96$. Most of the spin-up electrons come out of the structure from Contact 1, while most of the spin-down electrons are reflected by the potential barrier underneath the top gate (Fig. 4(a)). The spin-down electrons flow to the bottom channel along the right boundary of the structure in the flowing direction and come out from Contact 4. At point B, $P_{42} \approx 0.94$. Electrons cannot flow through the potential barrier underneath the top gate and are entirely reflected to the bottom channel. Again the spin-down electrons are mostly reflected by the potential barrier brought by the bottom gate and flow to Contact 3, while the spin-up electrons can flow through the potential and come out from Contact 4 (Fig. 4(b)).

In summary, we design a four-terminal nanostructure with two surface metal gates and show that it can serve as a spin splitter/switcher. In the ballistic transport regime, we utilize the gate-controlled potential barriers, combined with Zeeman splitting effect and edge current to control the spin freedom of the outputs. We show that by tuning the voltage of gates, the injected spin-unpolarized current can be split into different spin current with a high efficiency, and flow out of the geometry from different terminals. Furthermore, by

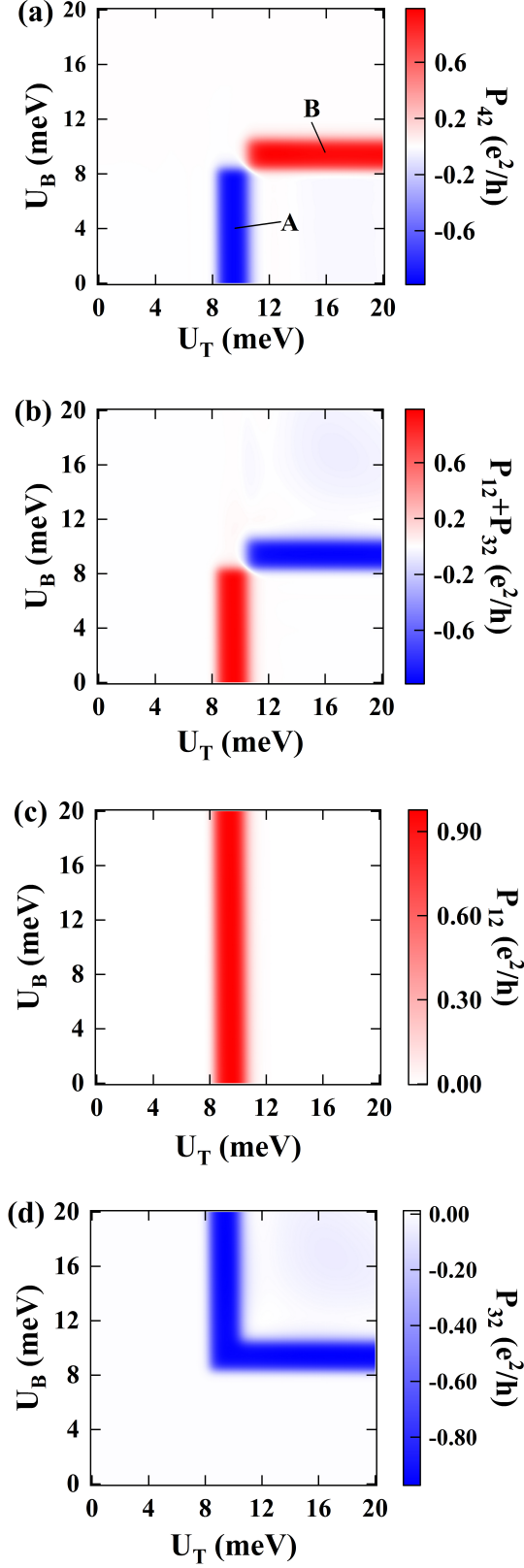


FIG. 3. (a) The conductance polarization P_{42} as the function of potential energy U_T and U_B . (b) The sum of conductance polarization P_{12} and P_{32} as the function of potential energy U_T and U_B . (c) The conductance polarization P_{12} as the function of potential energy U_T and U_B . (d) The conductance polarization P_{32} as the function of potential energy U_T and U_B . The magnetic strength is $B=1.5\text{T}$ in the $-z$ direction.

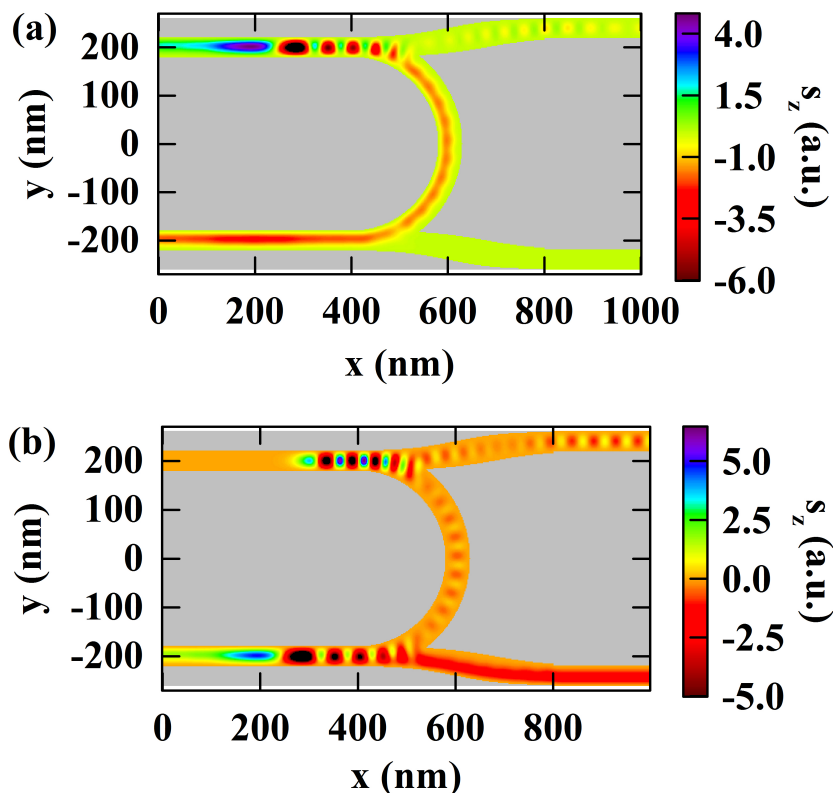


FIG. 4. (a) The total spin density s_z in the nanostructure for point A in Fig. 3(a). (b) The total spin density s_z in the nanostructure for point B in Fig. 3(a). The magnetic strength is $B=1.5\text{T}$ in the $-z$ direction.

tuning the voltage of gates, the outflow spin of one terminal can be switched.

This research was supported by the National Key R&D Program of China under Grant No. 2016YFF0200403 and the Key Program of National Natural Science Foundation of China under Grant No. 11234009.

¹S. Datta, and B. Das, Appl. Phys. Lett. **56**, 665 (1998).

²G. Schmidt, D. Ferrand, L. W. Molenkamp, A. T. Filip, and B. J. van. Wees, Phys. Rev. B **62**, R4790 (2000).

³T. Jungwirth, J. Sinova, J. Mašek, J. Kučera, and A. H. MacDonald, Rev. Mod. Phys. **78**, 809 (2006).

⁴R. Fiederling, M. Keim, G. Reuser, W. Ossau, G. Schmidt, A. Waag, and L. W. Molenkamp, Nature **402**, 787 (1999).

⁵J. A. Folk, R. M. Potok, C. M. Marcus, and V. Umansky, Science **299**, 679 (2003).

⁶M. P. Nowak and B. Szafran, Appl. Phys. Lett. **103**, 202404 (2013).

⁷M. Eto, T. Hayashi and Y. Kurotani, J. Phys. Soc. Jpn. **74**, 1934 (2005).

⁸I. V. Zozoulenko and M. Evaldsson, Appl. Phys. Lett. **85**, 3136 (2004).

⁹S. Komiyama, H. Hirai, S. Sasa and S. Hiyamizu, Phys. Rev. B **40**, 12566 (1989).

¹⁰J. H. Davis, I. A. Larkin and E. V. Sukhorukov, J. Appl. Phys. **77**, 4504 (1995).

¹¹C. W. Groth, M. Wimmer, A. R. Akhmerov and X. Waintal, New J. Phys. **16**, 063065 (2014).

¹²S. Datta, Electronic Transport in Mesoscopic Systems (Cambridge University Press, 1995).